

## Contrasting brain patterns of writing-related DTI parameters, fMRI connectivity, and DTI–fMRI connectivity correlations in children with and without dysgraphia or dyslexia



T.L. Richards<sup>a,\*</sup>, T.J. Grabowski<sup>a</sup>, P. Boord<sup>a</sup>, K. Yagle<sup>a</sup>, M. Askren<sup>a</sup>, Z. Mestre<sup>a</sup>, P. Robinson<sup>a</sup>, O. Welker<sup>a</sup>, D. Gulliford<sup>a</sup>, W. Nagy<sup>b</sup>, V. Berninger<sup>c</sup>

<sup>a</sup>Integrated Brain Imaging Center, Department of Radiology, University of Washington, Seattle, USA

<sup>b</sup>Department of Education, Seattle Pacific University, Seattle, USA

<sup>c</sup>Department of Educational Psychology, University of Washington, Seattle, USA

### ARTICLE INFO

#### Article history:

Received 5 June 2014

Received in revised form 10 March 2015

Accepted 10 March 2015

Available online 28 March 2015

#### Keywords:

Dyslexia

Dysgraphia

Connectivity

fMRI

DTI

### ABSTRACT

Based on comprehensive testing and educational history, children in grades 4–9 (on average 12 years) were diagnosed with dysgraphia (persisting handwriting impairment) or dyslexia (persisting word spelling/reading impairment) or as typical writers and readers (controls). The dysgraphia group ( $n = 14$ ) and dyslexia group ( $n = 17$ ) were each compared to the control group ( $n = 9$ ) and to each other in separate analyses. Four brain region seed points (left occipital temporal gyrus, supramarginal gyrus, precuneus, and inferior frontal gyrus) were used in these analyses which were shown in a metaanalysis to be related to written word production on four indicators of white matter integrity and fMRI functional connectivity for four tasks (self-guided mind wandering during resting state, writing letter that follows a visually displayed letter in alphabet, writing missing letter to create a correctly spelled real word, and planning for composing after scanning on topic specified by researcher). For those DTI indicators on which the dysgraphic group or dyslexic group differed from the control group (fractional anisotropy, relative anisotropy, axial diffusivity but not radial diffusivity), correlations were computed between the DTI parameter and fMRI functional connectivity for the two writing tasks (alphabet and spelling) by seed points. Analyses, controlled for multiple comparisons, showed that (a) the control group exhibited more white matter integrity than either the dysgraphic or dyslexic group; (b) the dysgraphic and dyslexic groups showed more functional connectivity than the control group but differed in patterns of functional connectivity for task and seed point; and (c) the dysgraphic and dyslexic groups showed different patterns of significant DTI–fMRI connectivity correlations for specific seed points and written language tasks. Thus, dysgraphia and dyslexia differ in white matter integrity, fMRI functional connectivity, and white matter–gray matter correlations. Of clinical relevance, brain differences were observed in dysgraphia and dyslexia on written language tasks yoked to their defining behavioral impairments in handwriting and/or in word spelling and on the cognitive mind wandering rest condition and composition planning.

© 2015 The Authors. Published by Elsevier Inc. This is an open access article under the CC BY-NC-ND license (<http://creativecommons.org/licenses/by-nc-nd/4.0/>).

### 1. Introduction

Dysgraphia is a word of Greek origin that means the condition (-ia) of impaired (dys) graph (letter produced by hand). Dyslexia is a word of Greek origin that means the condition (-ia) of impaired (dys) word (lex from lexicon, the mental dictionary). Thus, dysgraphia and dyslexia differ in the level of written language impairment—subword (letter) or word (oral decoding in reading or written encoding in spelling).

Pioneering research showed that although dyslexia is thought to be a reading disability, spelling disability is the persisting problem in

dyslexia across the life span (Lefly, and Pennington, 1991; Bruck, 1993; Connelly et al., 2006); and spelling disability is now used to define dyslexia in many languages including those with transparent orthographies for decoding (Schulte-Körne, 1998). However, more brain imaging research on dyslexia has used phonological or word decoding tasks (e.g., judgments about rhymes, phonemes, grapheme-phoneme correspondences) than spelling tasks. The word-specific spelling task used in much behavioral research on dyslexia (Olson et al., 1994) – select among the choices, all of which sound like a real word when pronounced, the one that is a correctly spelled word – has been studied during separate fMRI BOLD studies in children with developmental dyslexia (Richards et al., 2006) or with developmental dysgraphia (Richards, 2009). In both studies participants (in grades 4–6 or grade

\* Corresponding author.

E-mail address: [toddr@uw.edu](mailto:toddr@uw.edu) (T.L. Richards).

5, respectively) had persisting spelling problems despite extra help in the early grades, but different clinical profiles (impaired spelling and word decoding in dyslexia; and impaired handwriting, which interfered with spelling, but no reading problems in dysgraphia). In both these studies the same word-specific spelling task was used, but children with dyslexia or dysgraphia differed significantly from controls in BOLD activation in different regions of interest (ROIs), providing initial evidence for different brain bases for spelling problems in dyslexia and dysgraphia.

Although there have been imaging studies for the handwriting problems in dysgraphia (Richards, 2011), brain imaging studies of developmental dyslexia typically do not assess handwriting during scanning. The current imaging study extended these prior studies by comparing dysgraphic and dyslexic groups in the same study and on both a handwriting and spelling task, each of which had a common response requirement—production of a single letter. However, in contrast to the two prior studies that used a word-specific spelling judgment task (yes or no decision about whether a letter string is a correctly spelled word), the current study required the creation of a word-specific spelling by writing a missing letter in the blank in a letter series to create the correctly spelled word. Also in contrast to the prior handwriting study on dysgraphia in which the task was to write a familiar letter or pseudoletter equated on nature and number of strokes, in the current study the alphabet writing task required writing the letter that comes next in the alphabet after the visually displayed letter.

Thus, the five research aims of the current study were to extend prior brain imaging studies of the writing problems in developmental dysgraphia and developmental dyslexia. The first aim was to compare children with dysgraphia to controls, children with dyslexia to controls, and children with dysgraphia to children with dyslexia in the same study. The second aim was to make each of these comparisons on both handwriting and spelling tasks. However, to keep the response requirements constant for the handwriting and spelling tasks, each required production of a single letter and the correct letters were kept constant across the tasks. What varied was the processing that led to the letter production—whether the task required finding, retrieving, and producing a letter from the ordered alphabet series in memory (subword access) or supplying a missing letter in a letter sequence to create a word-specific spelling (lexical access). The third aim was to make each of these group comparisons on cognitive tasks as well as writing tasks because writing involves cognitive processes such as idea flow (Kellogg, 1994) and strategic planning for composing (Hayes, 1996) and not just language.

The fourth aim was to investigate four indices of white matter integrity relevant to structural connectivity and fMRI functional connectivity from four seed points shown in a metaanalysis to be associated with written word production (Purcell, 2011), thus moving beyond a region-of-interest (ROI) comparison on BOLD activation as in the prior word-specific spelling studies, or only structural connectivity (Vandermosten, 2012; Klingberg, 2000) or only functional connectivity (Richards and Berninger, 2008) in spelling or spelling-related skills. The fifth aim was to draw on paradigm changes in brain imaging research related to the human connectome (Bullmore and Sporns, 2009; Smith, 2013; van den Heuvel and Sporns, 2011; Markov et al., 2013a; Markov et al., 2013b). Of interest were contrasting complex patterns of differences between the control and each diagnostic group and between the two diagnostic groups on multiple indices of white matter integrity, which have implications for structural connectivity, and functional fMRI connectivity, and correlations between DTI and fMRI connectivity, which have implications for the white matter–gray matter relationships. Prior imaging research has correlated DTI and fMRI BOLD for regions of interest (Olesen, 2003; Vaden et al., 2015); the current study extended that approach by correlating DTI parameters with fMRI functional connectivity.

As in the prior studies of word-specific spelling judgments and writing real letters and pseudoletters, participants were in upper

elementary school or middle school and had to meet evidence-based criteria for dysgraphia or dyslexia on clinical measures (Berninger and Richards, 2010) and demonstrate persisting struggles with handwriting (dysgraphia) or word reading and spelling (dyslexia). Because the current study was grounded in prior behavioral and brain studies of developmental dysgraphia and dyslexia, two a priori hypotheses were tested.

The first hypothesis was that the dysgraphic and dyslexic groups would differ in fMRI functional connectivity from the controls and from each other on the second and third tasks, both of which are written language tasks that differ in the level of language that is impaired—subword letter only or letter in word context. In addition, they would show contrasting patterns of DTI–functional connectivity correlations for the two written language tasks (alphabet writing and filling in blank to create word-specific spelling).

The second hypothesis was that the dysgraphic and dyslexic groups, whose cognitive ability on a psychometric measure fell within the normal range, would not differ on either the first cognitive process (idea flow) (Kellogg, 1994), as assessed during mind wandering on the resting condition (Raichle, 2001), or the second cognitive process (planning) (Hayes, 1996), as assessed by idea generation before composing outside the scanner (Berninger, 2009). The rationale was that even though cognitive processes are involved in writing, it is the written language impairments at the subword or word level that define dysgraphia or dyslexia.

To summarize, in the current study we compared groups of children in grades 4–9 without dysgraphia or dyslexia with children carefully diagnosed as having dysgraphia or dyslexia. At issue is whether their neurological profiles of white matter integrity, functional connectivity, and white matter–gray matter correlations are the same or different on handwriting and spelling tasks. Showing that they differ not only in behavioral patterns (profiles of clinical measures) but also on brain patterns relevant to white matter, gray matter, and their interrelationships would provide interdisciplinary construct validity that dysgraphia and dyslexia are different kinds of specific learning disabilities (SLDs).

## 2. Materials and methods

### 2.1. Participants

Participants in grades 4–9 were recruited through local schools that referred students who despite extensive extra help in the early grades both at school and outside school continued to struggle with writing and/or reading. The children completed an extensive battery of comprehensive assessment and their parents completed numerous questionnaires about developmental, medical, family, and educational history. All had Verbal Comprehension Index scores that fell at least within the normal range (80 and above). The three groups differed significantly on two standardized measures of handwriting (Barnett et al., 2007) and two standardized measures of spelling (Mather et al., 2008; Pearson, 2009). These measures were corroborated with parent-reported histories of no struggles with learning to read or write (control group), ongoing struggles with handwriting but not reading (dysgraphia group) or spelling and word decoding/reading (dyslexia group): *DASH Copy Sentence in Best Writing*,  $F(2, 35) = 5.73$ ,  $p = .007$ , *DASH Copy Sentence in Fast Writing*,  $F(2, 34) = 8.20$ ,  $p < .001$ , *WIAT 3 Spelling Dictated Words*,  $F(2, 34) = 8.20$ ,  $p < .001$ , and *TOC Sight Spelling* (choosing correctly spelled real word),  $F(2, 34) = 13.20$ . One severely impaired student could not complete the last three measures, which accounts for the difference in degrees of freedom. The means for each measure (see Table 1) show that controls always scored higher, with the dysgraphic group more impaired than the dyslexic group on both handwriting measures and the dyslexic group more impaired than the dysgraphic group on both spelling measures.

40 participants met research inclusion criteria, were right handed, and did not wear metal that could not be removed. They participated in the imaging study (15 females, 25 males, age,  $M = 12$  years 3 months,

**Table 1**  
Significant differences among the groups on two handwriting and two spelling measures.

	Controls	Dysgraphics	Dyslexics	(df)	F	p
DASH Copy Best	11.33 (3.64)	6.64 (3.32)	7.53 (3.20)	(2, 35)	5.73	.007
DASH Copy Fast	9.83 (3.12)	5.07 (2.20)	6.20 (2.93)	(2, 34)	8.20	.001
WIAT3 Spelling	109.33 (13.77)	98.08 (17.46)	86.21 (8.94)	(2, 34)	8.20	.001
TOC Sight Spelling	12.56 (1.13)	10.38 (2.72)	8.21 (1.89)	(2, 34)	13.20	.001

Note. All these normed measures are on a scale of  $M = 10$ ,  $SD = 3$  (<6: below average, 6–7: low average, 8–11: average, 12–13: above average), except WIAT3 Spelling,  $M = 100$ ,  $SD = 15$  (80–89: low average, 90–109: average).

range 9 years-0 months to 15 years-2 months). They had been assigned, based on both test results and parent questionnaires documenting history of persisting struggle in subword handwriting or word reading and spelling to one of three groups using evidence-based criteria (Berninger and Richards, 2010): (1) typically developing control ( $n = 9$ , of which 5 were females), (2) dysgraphia ( $n = 14$ , of which 3 were females), or (3) dyslexia ( $n = 17$  of which 7 were females). Although gender was not well-matched across groups, the effect of gender was controlled by using gender as a covariate in the analyses.

## 2.2. Tasks during scanning

It was possible to study writing during imaging by using a novel MRI-compatible stylus, which allows participants to write while in the scanner and stores what they write concurrently and is registered in time with the fMRI data acquisition for subsequent analyses (Reitz, 2013). Each participant received training outside the scanner and completed four tasks in this order: (a) no experimenter-defined task (RESTING STATE), (b) production of the letter that follows a visually displayed letter in alphabet order (ALPHABET WRITING task), (c) production of letter in the blank in a visually displayed letter string to create a correctly spelled word (SPELLING WRITING task), and (d) planning a composition on an experimenter-provided topic (PLANNING task).

The resting condition lasted for 6 min 14 s. It was followed by 6 s of instruction for the alphabet task. The alphabet writing task lasted for 4 min and was self-paced. After the visual display of the first letter, the child wrote the next letter in the alphabet. When the child lifted the pen off the tablet then visual display 2 appeared and the process repeated until the 4 min was complete. Next there were 6 s of instruction for spelling followed by the spelling task that lasted for 4 min and was self-paced. After visual display 1, the child wrote a letter in the blank to complete the word spelling. When the child lifted the pen off the tablet, visual display 2 appeared and the process repeated until the 4 min was complete. Next, instructions for planning stayed on the screen for the whole 4 min, while the child just generated ideas and planned a composition on topic provided but did no writing until leaving the scanner. The instructions provided a topic and purpose for the composition (writing advice for an astronaut during space travel). The response requirement was the same for the alphabet and spelling tasks—to form one letter using the MRI-compatible stylus. However, the language tasks differed in the level of language that had to be accessed during processing and letter production—single subword letter in ordered alphabet series or single lexical unit. During the fMRI writing tasks, a mirror system enabled the participant in the scanner to see the instructions and task on a screen. The tasks and writing pad recordings were all programmed, timed, and coordinated with the scanner triggers using E-prime and in-house LabView software.

## 2.3. Data acquisition

Diffusion tensor imaging (DTI) scans and functional magnetic resonance imaging (fMRI) connectivity scans were obtained for all 40 children on a Philips 3 T Achieva scanner (release 3.2.2 with the 32-channel head coil) to obtain measures of structural white matter integrity and functional connectivity, respectively. All scans were acquired at the Diagnostic Imaging Sciences Center in collaboration with the

Integrated Brain Imaging Center and had Institutional Review Board approval. Each participant was screened for MRI safety before entering the scanner. Physiological monitoring was performed using the Philips pulse oximeter placed on the left hand index finger for cardiac recording; and respiration was recorded using the Philips bellows system where the air-filled bellows pad was placed on the abdomen. Head-immobilization was aided by using an inflatable head-stabilization system (Crania, Elekta).

The following MRI series were scanned: 1) 3-plane scout view with gradient echo pulse sequence: TR/TE 9.8/4.6 ms; Field of view  $250 \times 250 \times 50$  mm; acquisition time 30.3 s; 2) reference scan (used in parallel imaging) with gradient echo pulse sequence: TR/TE 4.0/0.75 ms; Field of View  $530 \times 530 \times 300$  mm; acquisition time 44.4 s; 3) Resting State fMRI scan with echo-planar gradient echo pulse sequence (single shot): TR/TE 2000/25 ms; Field of view  $240 \times 240 \times 99$  mm; slice orientation transverse, acquisition voxel size  $3.0 \times 3.08 \times 3.0$  mm; acquisition matrix  $80 \times 80 \times 33$ ; slice thickness 3.0, SENSE factor in the AP direction 2.3; epi factor 37; bandwidth in the EPI frequency direction 1933 Hz, SoftTone factor 3.5, sound pressure 6.1 dB, 180 dynamic scans; 5 dummy scans; fold over direction AP, acquisition time 6:14 min/s; 4) B0 field map imaging with gradient echo pulse sequence and 2 echos; TR/TE 11/6.3 ms; delta TE 1.0 ms; slice orientation transverse, Field of view  $240 \times 240 \times 129$  mm; voxel size  $1.5 \times 1.5 \times 3.0$  mm; acquisition matrix  $160 \times 160 \times 43$ , output image magnitude and phase, acquisition time 2:29 min/s; 5) MPRAGE structural scan: TR/TE 7.7/3.5 ms, Field of view  $256 \times 256 \times 176$  mm, slice orientation sagittal, voxel size  $1 \times 1 \times 1$  mm, inversion pulse delay 1100 ms, Sense factor 2 in the AP direction, acquisition time 5:33 min/s; 6) diffusion tensor imaging with echo-planar spin-echo diffusion pulse sequence: TR/TE 8593/78 ms, slice orientation transverse, Field of view  $220 \times 220 \times 128$  mm, voxel size  $2.2 \times 2.2 \times 2.0$  mm, bvalues 0 and 1000, output images 1 bvalue at 0 and 32 bvalues at 1000 with 32 different diffusion vector non-colinear directions, SoftTone factor 4.0, sound pressure 3.1 dB, bandwidth in the EPI frequency direction 1557.7 Hz, epi factor 57, acquisition time 9:35.7 min/s; and 7) fMRI during the writing tasks: same parameters as with the Resting State fMRI described above except with dynamic scans 387, acquisition time 13:08 min/s.

## 2.4. Diffusion tensor imaging analysis

DTI data were processed with DTIPrep/GTRACT software to ensure quality control and generate the tensors (<http://www.nitrc.org/projects/dtiprep/>). Then custom software (GFORTAN) was used to calculate the DTI parameters (fractional anisotropy, axial diffusivity, radial diffusivity, relative anisotropy, mean diffusivity) from the tensors. FSL software (tract-based spatial statistics, TBSS) was used to co-register and prepare the DTI data for group analysis using a higher level design matrix to perform a voxel by voxel group map comparison between groups. FSL's randomise software, which robustly corrects for multiple comparisons with permutation methods in <http://fsl.fmrib.ox.ac.uk/fsl/fslwiki/TBSS/UserGuide> (see "Threshold-Free Cluster Enhancement" TFCE option), was used to generate the group maps, which were co-registered to the FSL standard white matter atlas called FHU. A regional analysis was performed within each significant cluster, for example, FSL's cerebellum atlas for cerebellar regions.

Fractional anisotropy (FA, i.e., an index of the amount of anisotropy) is used as an index of white matter integrity; greater FA is associated with increased myelination (Wheeler-Kingshott et al., 2009; Mori, 2007). Relative anisotropy (RA) is a lesser-known DTI measure of anisotropy that gives different information than FA as described by Basser and Pierpaoli (1996). The exact equation for RA is shown here:

$$RA = \sqrt{\lambda_1 - \lambda^2 + \lambda_2 - \lambda^2 + \lambda_3 - \lambda^2} / \sqrt{3[\lambda]^2}$$

where RA is the relative anisotropy, and  $\lambda_1$ ,  $\lambda_2$ , and  $\lambda_3$  are the three eigenvalues resulting from the tensor calculation and  $[\lambda]$  is the mean  $\lambda$  which is  $(\lambda_1 + \lambda_2 + \lambda_3) / 3$ . Water molecules in the brain's white fiber tracts are more likely to be anisotropic. Anisotropy is dependent on the strength of connectivity in one direction in contrast to isotropy that applies in all directions. Fractional anisotropy (FA) describes the degree to which the diffusion is isotropic (value of 0) or anisotropic (higher value up through 1). Relative anisotropy (RA) is the ratio of the anisotropic part of tensor D to its isotropic part. The diffusivity in directions perpendicular to the principal axis of diffusion (radial diffusivity) has been associated with the degree of myelination and number of branching, exiting fibers, whereas diffusivity along and parallel to the principal axis (axial diffusivity) has been associated with the axon diameter (Song, 2002; Song, 2005), but see (Mori, 2007) for a critical interpretation of these indices.

The DTI data were also analyzed using a seed point connectivity analysis, using seeds from a published metaanalysis (Purcell, 2011) to generate group maps for the 3 groups (controls, dysgraphics and dyslexics) for 4 different seed points (left precuneus cortex, left temporooccipital cortex, left supramarginal cortex, and left inferior frontal gyrus). FSL's probabilistic tractography and bedpost software were used to generate the tracts which were connected to the seed regions.

## 2.5. Functional connectivity analysis

Functional images were corrected for motion using FSL MCFLIRT (Jenkinson et al., 2002), and then high-pass filtered at  $\sigma = 20.83$ . Motion scores (as given in the MCFLIRT report) were computed for each subject and average motion score (mean absolute displacement) for each of the groups: control  $1.31 \pm 1.37$  mm, dysgraphic  $1.50 \pm 1.23$  mm, and dyslexic  $1.47 \pm 1.03$  mm. Spikes were identified and removed using the default parameters in AFNI's 3dDespike. Slice-timing correction was applied with FSL's slicetimer and spatial smoothing was performed using a 3D Gaussian kernel with FWHM = 4.0 mm. Time series motion parameters and the mean signal for eroded (1 mm in 3D) masks of the lateral ventricles and white matter (derived from running FreeSurfer's recon-all on the T1-weighted image) were analyzed. Co-registration of functional images to the T1 image was performed using boundary based registration based on a white matter segmentation of the T1 image through `epi_reg` in FSL. The MPRAGE structural scan was segmented using FreeSurfer software; white matter regressors were used to remove unwanted physiological components. The same seed points as used in DTI were also used in fMRI connectivity (Purcell, 2011).

## 2.6. DTI–fMRI functional connectivity correlations

DTI/fMRI connectivity correlations were performed by extracting the exact DTI parameter value from each individual subject at the place in the brain where there was highest significance for the DTI results shown in Tables 2 and 6. Then the DTI values were demeaned and placed in the correlation design matrix using FSL higher level GLM guidelines. FSL software `randomise` compares DTI with fMRI connectivity for each of the seed points meeting the criteria described above.

## 2.7. Anatomy/atlas reports

The DTI structural and fMRI functional connectivity scans were then analyzed with reference to a brain atlas based on quantitative

analyses of 10 postmortem brains (Toga, 2006) in order to identify the cortical regions corresponding to the significant clusters. Cytoarchitectonic maps were used to identify patterns of connectivity within parietal regions (Caspers, 2013). The Jülich histological (cyto- and myeloarchitectonic) atlas (Eickhoff, 2006; Eickhoff, 2007) and Eickhoff's Anatomy Toolbox (Eickhoff, 2007; Eickhoff, 2005) were used to identify patterns of connectivity throughout the brain for 32 gray matter and 10 white matter structures.

## 2.8. Data analyses

For all analyses, Oxford's fMRIB software library (FSL) "randomise", which performs permutations and threshold-free cluster enhancement, was used to control for multiple comparisons. A global design matrix was used as part of the GLM model in software `randomise` to make the group statistical comparisons as describe by FSL guidelines for higher group level analysis as show by this weblink [http://fsl.fmrib.ox.ac.uk/fsl/fslwiki/GLM#Two-Group\\_Difference\\_Adjusted\\_for\\_Covariate](http://fsl.fmrib.ox.ac.uk/fsl/fslwiki/GLM#Two-Group_Difference_Adjusted_for_Covariate). This model compared the groups with a gender covariate.

The first set of analyses focused on which of the four DTI indices (FA, RA, AD, RD) for each of the four seed points differentiated the dysgraphic and dyslexic groups from the control group and each other. The number and patterns of probabilistic tractography connections from DTI analyses, and pixel counts for group connectivity score clusters for structural white matter integrity connections were computed for each of the four seed points and three groups.

The second set of analyses focused on which of the fMRI connectivity results for each of the four seed points and four tasks differentiated the dysgraphic and dyslexic groups from the control group and from each other. Group maps for fMRI functional connectivity were generated for the 3 groups (control dysgraphic and dyslexic) for 4 different seed points in the left precuneus cortex PCC, in the left temporooccipital cortex TOC, in the left supramarginal gyrus SMG, and in the left inferior frontal gyrus, IFG Broca's area, based on a meta-analysis for written word production (Purcell, 2011), for each of the three writing tasks and resting condition. Brain activation during rest is sensitive to mind wandering (Raichle, 2001), whereas during planning for a topic defined by others, brain activation is sensitive to goal-related strategies (Hayes, 1996). fMRI time-series were averaged within regions of interest (ROIs) formed from a 15 mm sphere centered at each seed. The averaged time-series at each ROI was correlated with every voxel throughout the brain to produce functional connectivity correlation maps, converted to z-statistics using the Fisher transformation.

The third set of analyses computed correlations for DTI values extracted from the control versus dysgraphic group or control versus dyslexic group and fMRI functional connectivity for specific seed points and tasks. The goal was to identify, for DTI parameters shown to differentiate the dysgraphic or dyslexic group from controls, significant correlations between white matter integrity parameters and gray matter connectivity values, and then to compare patterns of significant DTI–fMRI connectivity correlations between the dysgraphic and dyslexic groups.

## 3. Results

### 3.1. Findings related to structural connectivity

The control group had higher fractional anisotropy (FA) than the dysgraphia group in the bilateral anterior thalamic radiation, left cingulum, and forceps minor. See Table 2 section A. The control group also had higher relative anisotropy (RA), which is another DTI parameter to measure anisotropy, than the dysgraphia group in each of those same four regions plus the left cortical spinal tract and bilateral superior longitudinal fasciculus (SLF). See Table 2 section B.

The brain regions where controls had higher RA values than the group with dyslexia are shown in Table 2 section C. Like the dysgraphia group, the dyslexia group had lower RA values than controls in the

**Table 2**  
Structural white matter integrity differences between control and dysgraphic groups, control and dyslexic groups, and dysgraphic and dyslexic groups.

A. Brain regions where controls had significantly higher values (corrected for multiple comparisons) than dysgraphics for DTI parameter FA (fractional anisotropy).			
Pixel count	Controls <i>M (SD)</i>	Dysgraphia <i>M (SD)</i>	Atlas label
18	0.442 (.057)	0.390 (.064)	L ant thal rad
5	0.408 (.044)	0.366 (.055)	R ant thal rad
93	0.471 (.096)	0.416 (0.101)	L cingulum
1203	0.611 (0.110)	0.550 (0.121)	Forceps minor
B. Brain regions where controls had significantly higher values (corrected for multiple comparisons) than dysgraphics for DTI parameter RA (relative anisotropy).			
Pixel count	Controls <i>M (SD)</i>	Dysgraphia <i>M (SD)</i>	Atlas label
26	105.524 (15.584)	93.198 (16.893)	L ant thal rad
147	128.934 (21.580)	115.378 (20.446)	R ant thal rad
139	130.941 (17.161)	116.921 (17.475)	L cort spinal
104	107.609 (22.716)	94.580 (23.544)	L cingulum
1433	160.816 (40.371)	143.269 (41.242)	Forceps minor
24	128.365 (26.722)	115.474 (21.141)	L SLF
43	111.143 (15.898)	90.895 (14.950)	R SLF
C. Brain regions where controls had significantly higher values (corrected for multiple comparisons) than dyslexics for DTI parameter RA (relative anisotropy).			
Pixel Count	Controls <i>M (SD)</i>	Dysgraphia <i>M (SD)</i>	Atlas label
141	83.535 (14.394)	74.588 (14.458)	L ant thal rad
473	128.883 (21.936)	115.917 (21.470)	R ant thal rad
187	120.176 (20.364)	107.279 (17.858)	R cort spinal
103	103.271 (16.919)	92.900 (15.213)	L cingulum
483	134.160 (33.334)	120.343 (32.349)	Forceps minor
157	85.534 (14.808)	76.137 (15.874)	L IFOF
36	117.307 (16.208)	102.249 (16.250)	R IFOF
19	72.882 (17.442)	65.368 (16.600)	L SLF
611	98.370 (20.835)	84.834 (18.186)	R SLF
167	106.912 (23.038)	92.969 (24.370)	L uncinate
41	105.433 (22.036)	91.032 (22.439)	R uncinate
D. Brain regions where controls had significantly higher values (corrected for multiple comparisons) than dyslexics for DTI parameter axial diffusivity (parallel diffusion).			
Pixel count	Controls <i>M (SD)</i>	Dysgraphia <i>M (SD)</i>	Atlas label
634	11.327 (1.071)	10.753 (1.039)	R ant thal rad
14	11.770 (1.134)	11.347 (1.058)	L cort spinal
401	11.303 (0.872)	10.759 (0.825)	R cort spinal
7	10.754 (0.400)	10.274 (0.845)	R cingulum
183	10.261 (0.782)	9.783 (0.792)	R IFOF
1084	10.181 (0.943)	9.524 (0.933)	R SLF
127	11.559 (0.702)	11.023 (0.732)	R uncinate
E. Brain regions where dysgraphics had significantly higher values (corrected for multiple comparisons) than dyslexics for DTI parameter radial diffusivity (perpendicular diffusion).			
Pixel count	Dysgraphia <i>M (SD)</i>	Dyslexia <i>M (SD)</i>	Atlas labels
73	7.752 (1.115)	7.111 (0.931)	L ant thal rad
43	4.892 (0.733)	4.505 (0.743)	L cort spinal
446	6.840 (0.770)	6.334 (0.663)	L IFOF
22	6.726 (0.680)	6.312 (0.651)	L ILF
107	6.829 (0.643)	6.432 (0.562)	L SLF
41	6.726 (0.665)	6.248 (0.564)	L uncinate
8	6.570 (0.559)	6.161 (0.377)	L SLF temp

bilateral anterior thalamus radiation and SLF, left cingulum, and forceps minor. However, whereas only the dysgraphia group had lower values than the control group in left cortical spinal tract (see Table 2 section B), only the dyslexia group had lower values than the control group in the right cortical spinal, bilateral inferior frontal occipital, and bilateral uncinate tracts. The brain regions where the control group had higher values of axial diffusivity (AD), a measure of parallel diffusion, than the dyslexia group, are shown in Table 2 section D. Compared to the control group, the dyslexic group had lower parallel diffusivity in the bilateral cortical spinal tract, and right anterior thalamus radiation, cingulum, inferior frontal occipital tract, SLF, and uncinate.

As shown in Table 2 section E, the dysgraphic and dyslexic groups differed in radial diffusivity (RD), which is a measure of perpendicular diffusion. Compared to the dyslexia group, the dysgraphia group had higher RD in seven left hemisphere white-matter fiber tracts: anterior thalamus radiation, corticospinal, inferior frontal occipital fasciculus, inferior longitudinal fasciculus, superior longitudinal fasciculus, uncinate, and superior longitudinal fasciculus. Whereas RD differences were mainly found on the right for the dyslexia group versus the control

group, RD differences were mainly found on left for the dysgraphic group versus the dyslexic group.

### 3.2. Findings related to functional connectivity

As shown in Table 3, the dysgraphia group showed greater functional connectivity than the control group only during the planning for composing task for three of the seed points but not for the left supramarginal gyrus seed point. The dysgraphia group did not differ from the control group during resting condition (mind wandering without another-imposed task) (Raichle, 2001). In contrast, the dyslexia group had stronger functional connectivity than the control group during resting state (mind wandering) and always in the left-occipital temporal gyrus, consistent with dyslexics' problems in self-regulation of processes involved in written word spelling (Berninger and Richards, 2010), but not during planning. As shown in Table 4, the dysgraphia group did not differ from the control group on the two language production tasks, but the dyslexia group had greater functional connectivity than the control group, especially in the cerebellum, on both the alphabet letter writing and

**Table 3**

Seed points where functional connectivity for control group is significantly less (corrected for multiple comparisons) than for dysgraphic group or dyslexic group in specific seed points for the two cognitive writing tasks (flow on resting state and planning before composing). **Note.** No findings for control group < dysgraphic group on resting state or control group < dyslexic group on planning before composing.

A. Writing planning—control group < dysgraphia group.			
Left occipital-temporal seed point.			
Pixel count	Control <i>M</i> ( <i>SD</i> )	Dysgraphic <i>M</i> ( <i>SD</i> )	Atlas labels
58	−0.516 (2.031)	2.693 (2.580)	L Broca’s_area_BA44
11	1.802 (1.785)	4.684 (2.455)	L Visual_cortex_V4
7	0.548 (1.275)	2.875 (2.334)	L cerebel_Left_I-IV
8	0.382 (1.181)	2.765 (1.738)	cerebel_Right_I-IV
38	1.422 (1.953)	3.985 (2.496)	cerebel_Left_V
23	1.289 (1.595)	3.929 (2.311)	cerebel_Right_V
484	1.608 (1.937)	4.918 (2.883)	cerebel_Left_VI
115	1.687 (1.814)	5.196 (2.837)	cerebel_Vermis_VI
471	1.447 (1.713)	4.498 (2.652)	cerebel_Right_VI
516	1.826 (2.231)	4.749 (2.766)	cerebel_Left_Crus_I
693	1.20 (1.760)	3.945 (2.753)	cerebel_Right_Crus_I
9	0.870 (2.950)	3.508 (2.131)	cerebel_Left_Crus_II
80	0.260 (1.302)	2.272 (2.307)	cerebel_Right_Crus_II
5	0.874 (1.481)	2.678 (2.156)	cerebel_Left_VIIb
10	0.566 (1.283)	2.649 (2.595)	cerebel_Right_VIIb
22	0.674 (1.519)	2.695 (2.169)	cerebel_Left_VIIIa
39	0.728 (1.245)	3.260 (2.490)	cerebel_Vermis_VIIIa
54	0.359 (1.206)	2.233 (2.260)	cerebel_Right_VIIIa
19	0.478 (1.198)	2.840 (2.80)	cerebel_Vermis_VIIIb
Left precuneus seed point.			
Pixel count	Control <i>M</i> ( <i>SD</i> )	Dysgraphic <i>M</i> ( <i>SD</i> )	Atlas labels
283	0.054 (1.103)	2.470 (2.003)	cerebel_Right_Crus_I
79	−0.162 (0.787)	2.247 (2.177)	cerebel_Right_Crus_II
Left IFG Broca’s seed point.			
Pixel count	Control <i>M</i> ( <i>SD</i> )	Dysgraphic <i>M</i> ( <i>SD</i> )	Atlas labels
65	1.111 (1.783)	3.899 (2.965)	L_inferior_parietal_lobule_PF
43	1.787 (1.942)	4.559 (2.477)	L_inferior_parietal_lobule_PFcM
26	1.310 (1.826)	4.263 (2.751)	L_inferior_parietal_lobule_PFM
14	1.437 (1.738)	4.133 (2.892)	L_inferior_parietal_lobule_Pga
53	0.464 (1.526)	3.166 (2.506)	L_inferior_parietal_lobule_PGp
21	0.303 (0.990)	2.199 (2.159)	L_Visual_Cortex_V2_BA18
16	0.174 (1.248)	2.144 (2.071)	L_Visual_Cortex_V3V
84	−0.097 (1.688)	2.078 (2.219)	L_Visual_Cortex_V4
37	0.003 (1.968)	2.568 (2.367)	L_Visual_Cortex_V5
33	0.264 (1.253)	2.706 (2.462)	cerebel_Left_VI
7	0.471 (1.488)	2.588 (2.277)	cerebel_Vermis_VI
604	0.316 (1.307)	2.397 (2.279)	cerebel_Left_Crus_I
63	0.174 (1.150)	2.379 (2.404)	cerebel_Right_Crus_I
112	0.125 (1.167)	2.152 (2.174)	cerebel_Left_Crus_II
8	0.395 (1.283)	2.486 (2.437)	cerebel_Vermis_Crus_II
194	0.167 (1.253)	2.188 (2.217)	cerebel_Right_Crus_II
B. Resting state control group < dyslexia group.			
Left occipital-temporal seed point.			
Pixel count	Control <i>M</i> ( <i>SD</i> )	Dysgraphic <i>M</i> ( <i>SD</i> )	Atlas labels
22	6.901 (2.249)	1.924 (1.874)	cerebel_Left_Crus_I
6	3.837 (2.447)	0.796 (1.474)	cerebel_Vermis_VI
54	4.233 (1.631)	1.620 (1.831)	cerebel_Right_VI
198	4.394 (2.045)	1.503 (1.417)	cerebel_Left_Crus_I
301	4.620 (1.651)	1.646 (1.382)	cerebel_Right_Crus_I
26	3.970 (1.884)	1.175 (1.399)	cerebel_Left_Crus_II
20	3.476 (1.542)	0.987 (1.299)	cerebel_Vermis_Crus_II
16	4.756 (2.025)	1.695 (2.099)	cerebel_Right_Crus_II

spelling tasks. As shown in Table 5, the dyslexic group was over-connected compared to the dysgraphic group in the left inferior parietal lobe and primary and secondary somatosensory cortex.

Table 6 summarizes the total number of functionally connected voxels for the dysgraphic group and dyslexic group by seed points. For the alphabet writing task, the dysgraphia group had fewer functionally connected voxels than the dyslexia group from the left occipital temporal and left supramarginal gyri, but more functionally connected voxels from the left precuneus, a region common to both the default network and Rich

Club of the Human Connectome (Bullmore and Sporns, 2009; Smith, 2013; van den Heuvel and Sporns, 2011), than the dyslexia group. For the spelling writing task, the dyslexia group consistently had more functionally connected voxels for all four seed points than the dysgraphia group, consistent with dyslexia being associated with impaired word spelling. Table 6 also summarizes the number and patterns of probabilistic tractography connections from DTI analyses, and pixel counts for group connectivity score clusters for structural white matter integrity connections for each of the four seed points and three groups.

Synthesizing findings for functional connections across Tables 3, 4, 5, and 6 shows that the dysgraphic and dyslexic groups differed from the control group; but the dysgraphic and dyslexic groups do not necessarily differ in the same way (number and pattern) for each the four seed points or the four tasks/conditions. Indeed, when the dysgraphic and dyslexic groups were compared to each other, they often differed from each other as well.

**3.3. Contrasting dysgraphia and dyslexia DTI-fMRI functional connectivity correlations**

For each of the two written language tasks, correlations with fMRI connectivity were computed for each of the DTI parameters on which a diagnostic group differed significantly from the control group. All correlations were corrected for multiple comparisons. Only the significant correlations are reported.

For the dysgraphia group, there were significant positive correlations of DTI FA (fractional anisotropy values extracted from the control versus dysgraphic FA significant comparison) with fMRI functional connectivity from two seed points during the filling in the blank spelling task, with all correlations,  $p < .05$ . These correlations were found between the left supramarginal and 2 regions—left cingulum,  $r = 0.924$ , and to the cingulate gyrus, anterior division,  $r = .922$ , both  $p < .025$ ; and between the left inferior frontal (Broca’s area) and 3 regions—superior parietal lobule 7 aL,  $r = .850$ , to the superior frontal gyrus,  $r = .833$ , and to the precuneus cortex,  $r = .843$ .

For the dyslexia group, there were significant positive correlations of DTI RA (relative anisotropy values extracted from the control versus dyslexic group’s significant comparison) with fMRI functional connectivity from three seed points on the alphabet writing task and from two seed points on the filling in the blank spelling task, with all correlations  $p < .01$ . These correlations were found during the alphabet writing task, between left temporo-occipital and 10 other regions—Broca’s area right BA44,  $r = 0.860$ , right superior parietal lobule 7M,  $r = 0.864$ , left acoustic radiation,  $r = 0.895$ , corticospinal tract L0,  $r = .858$ , inferior frontal gyrus pars opercularis,  $r = 0.860$ , precentral gyrus,  $r = 0.861$ , postcentral gyrus,  $r = 0.853$ , lateral occipital cortex superior division,  $r = 0.849$ , paracingulate gyrus,  $r = 0.855$ , and precuneus cortex,  $r = .863$ . Correlations were also found between the left supramarginal gyrus and 4 other regions—left visual cortex V1/BA17,  $r = 0.867$ , intracalcarine cortex,  $r = 0.866$ , precuneus cortex,  $r = 0.864$ , and temporal fusiform cortex posterior division,  $r = 0.868$ ; and between the left inferior frontal gyrus (Broca’s area) and 7 regions—right inferior parietal lobule PF,  $r = 0.873$ , right inferior parietal lobule Pga,  $r = 0.868$ , right inferior parietal lobule PGp,  $r = 0.865$ , superior temporal gyrus posterior division,  $r = 0.869$ , postcentral gyrus,  $r = 0.859$ , angular gyrus,  $r = 0.865$ , and lingual gyrus,  $r = 0.854$ . During the fill in the blank spelling task, there were correlations between the left temporooccipital gyrus and 4 regions—left superior parietal lobule 7a,  $r = 0.861$ , left visual cortex V1/BA17,  $r = 0.855$ , lateral occipital cortex superior division,  $r = 0.858$ ; and cuneal cortex,  $r = 864$ ; and between the inferior frontal gyrus (Broca’s area) and 2 regions—right visual cortex V2/BA18,  $r = 0.858$ , and lingual gyrus,  $r = 0.858$ .

For the dyslexia group, there was also a significant positive correlation of DTI AD (axial diffusivity values extracted for each individual from a location where there was a significant difference between dyslexics and controls on DTI AD) with fMRI functional connectivity from one seed point on the alphabet writing task and from four seed points

**Table 4**  
Brain regions where functional connectivity for control group is significantly less (corrected for multiple comparisons) than for dyslexic group in specific seed points for ordered alphabet or word-specific spellings. Note: none for control group < dysgraphic group.

A. Letter production alphabet order task controls < dyslexics. Left occipital-temporal seed point.			
Pixel count	Control M (SD)	Dysgraphic M (SD)	Atlas labels
105	1.616 (1.680)	4.416 (1.823)	cerebel_Left_VI
17	1.934 (1.863)	4.802 (1.592)	cerebel_Vermis_VI
8	1.294 (1.665)	4.053 (1.408)	cerebel_Right_VI
5	0.926 (1.387)	4.225 (1.735)	cerebel_Right_Crus_I
B. Letter production in blank to spell word task control group < dyslexia group. Left occipital-temporal seed point.			
Pixel count	Control M (SD)	Dysgraphic M (SD)	Atlas labels
5	1.928 (1.697)	4.944 (1.872)	L_Visual_Cortex_V2_BA18
33	1.243 (1.758)	4.739 (1.926)	L_Visual_Cortex_V4
9	1.090 (1.384)	3.691 (1.934)	cerebel_Left_I-IV
29	0.791 (1.466)	3.153 (1.482)	cerebel_Right_I-IV
41	1.990 (1.986)	4.633 (1.782)	cerebel_Left_V
14	1.269 (1.837)	3.682 (1.731)	cerebel_Right_V
288	1.683 (1.997)	4.555 (2.054)	cerebel_Left_VI
45	2.056 (1.790)	5.240 (2.066)	cerebel_Vermis_VI
106	1.122 (1.635)	3.713 (2.131)	cerebel_Right_VI
57	1.448 (1.872)	4.711 (2.139)	cerebel_Left_Crus_I
199	0.888 (1.426)	3.822 (2.229)	cerebel_Right_Crus_I

on the filling in the blank spelling task. During the alphabet writing task, significant correlations were found between the left inferior frontal gyrus (Broca's area) and the middle temporal gyrus (temporooccipital part),  $r = .837, p < .02$ . During the fill in the blank spelling task, there were significant correlations found between the left tempoparietal gyrus and 21 other regions, all  $p < .01$ . These 21 regions were: left inferior parietal lobule PF,  $r = .834$ , left inferior parietal lobule PGp,  $r = .825$ , left superior parietal lobule 7a,  $r = .832$ , right superior parietal lobule 7a,  $r = .810$ , left superior parietal lobule 7M,  $r = .816$ , left superior parietal lobule 7p,  $r = .827$ , left visual cortex V2/BA 18,  $r = .815$ , right cingulum,  $r = .818$ , right corticospinal tract,  $r = .836$ , left corticospinal tract,  $r = .848$ , left inferior occipitofrontal fascicle,  $r = .808$ , right optic radiation,  $r = .835$ , left optic radiation,  $r = .823$ , right uncinate fascicle,  $r = .818$ , insular cortex,  $r = .821$ , posterior supramarginal gyrus,  $r = .833$ , angular gyrus,  $r = .839$ , superior lateral occipital cortex,  $r = .835$ , anterior cingulate gyrus,  $r = .815$ , precuneus cortex,  $r = .821$ , and cuneal cortex,  $r = .817$ ; from the left supramarginal to 3 regions, all  $p < .02$ —right premotor cortex BA6,  $r = .815$ , paracingulate gyrus,  $r = .825$ , and anterior cingulate gyrus,  $r = .814$ ; from the left precuneus to 3 regions, all  $p < .02$ —left visual cortex V2/BA 18,  $r = .850$ , precuneus cortex,  $r = .838$ , and occipital fusiform gyrus,  $r = .823$ ; and from the inferior frontal gyrus (Broca's area) to 12 regions, all  $p < .01$ —right anterior intraparietal sulcus hIP3,  $r = .831$ , left

visual cortex V1/BA 17,  $r = .829$ , left visual cortex V2/BA 18,  $r = .823$ , right visual cortex V2/BA 18,  $r = .819$ , right corticospinal tract,  $r = .819$ , left optic radiation,  $r = .814$ , lateral superior occipital cortex,  $r = .826$ , lateral inferior occipital cortex,  $r = .819$ , intracalcarine cortex,  $r = .829$ , lingual gyrus,  $r = .825$ , temporal occipital fusiform cortex,  $r = .833$ , and occipital fusiform gyrus,  $r = .826$ .

To summarize, for the dysgraphia group, the DTI FA-fMRI functional connectivity correlations were significant from two seed points on the fill in the blank spelling task. For the dyslexia group, the DTI RA-fMRI functional connectivity correlations were significant from three seed points on the alphabet writing task and from two seed points on the fill in the blank spelling task; and the DTI AD-fMRI functional connectivity correlations were significant from one seed point on the alphabet writing task and four seed points on the fill in the blank spelling task. Thus, the significant white matter-gray matter correlations varied by diagnostic group, DTI parameter, tasks, and seed points. For the dysgraphia group, these correlations were significant only for the DTI FA parameter and only for the fill in the blank spelling task. For the dyslexia group, these correlations were significant only for DTI RA and DTI AD, for both the alphabet writing task and the fill in the blank spelling task, but the patterns of seed point to region(s) for specific written language tasks varied with DTI parameter.

**Table 5**  
Seed points where functional connectivity is significantly less (corrected for multiple comparisons) for dysgraphics than for dyslexics on levels of language tasks. Letter production in blank to spell word task. Left occipital temporal Seed Point.

Letter production in blank to spell word task. Left occipital temporal seed point.			
Pixel count	Dysgraphic M (SD)	Dyslexic M (SD)	Atlas labels
21	1.237 (1.623)	3.524 (1.982)	L Inferior_parietal_lobule_PF
7	1.005 (1.309)	3.457 (2.379)	L Inferior_parietal_lobule_PFcM
10	0.808 (1.522)	3.094 (1.836)	L Inferior_parietal_lobule_PFop
51	0.804 (1.563)	2.848 (1.565)	L Inferior_parietal_lobule_PFt
13	2.024 (1.954)	4.978 (2.188)	L Inferior_parietal_lobule_Pga
7	0.602 (1.589)	2.660 (1.653)	L Primary_motor_cortex_BA4p
69	1.284 (1.620)	3.431 (1.832)	L Primary_somatosensory_cortex_BA1
49	1.385 (1.611)	3.681 (1.976)	L Primary_somatosensory_cortex_BA1
15	-0.103 (1.586)	2.015 (1.808)	L Primary_somatosensory_cortex_BA3a
92	0.694 (1.516)	3.030 (1.890)	L Primary_somatosensory_cortex_BA3b
42	0.181 (1.560)	2.568 (1.985)	L Second_somatosensory_cortex_OP1
58	0.521 (1.290)	2.648 (1.841)	L Second_somatosensory_cortex_OP4

**Table 6**

Number of functional connections, number of structural white matter integrity connections (probabilistic tractography), and pixel counts for group connectivity score clusters for structural white matter integrity connections in brains in control, dysgraphic, and dyslexic groups alone for the four seed points.

A1. Functional connections for resting state.			
Seed brain region	Control	Dysgraphic	Dyslexic
Left occipital temporal	67	98	74
Left supramarginal gyrus	77	117	102
Left precuneus	38	75	54
Left inferior frontal	61	94	83
A2. Functional connections for letter production alphabetic order.			
Seed brain region	Control	Dysgraphic	Dyslexic
Left occipital temporal	18	60	73
Left supramarginal gyrus	15	65	78
Left precuneus	21	55	46
Left inferior frontal	16	43	44
A3. Functional connections for letter production fill in blank to spell.			
Seed brain region	Control	Dysgraphic	Dyslexic
Left occipital temporal	19	23	77
Left supramarginal gyrus	33	64	85
Left precuneus	27	54	88
Left inferior frontal	17	34	48
A4. Functional connections for planning before composing.			
Seed brain region	Control	Dysgraphic	Dyslexic
Left occipital temporal	4	30	25
Left supramarginal gyrus	7	66	47
Left precuneus	15	67	34
Left inferior frontal	5	50	29
B. DTI probabilistic tractography.			
Seed brain region	Control	Dysgraphic	Dyslexic
Left occipital temporal	6	6	5
Left supramarginal gyrus	3	11	10
Left precuneus	17	6	6
Left inferior frontal	9	6	4
C. Structural white matter integrity connections values for four seed points.			
Left occipital temporal seed point.			
Subject group	Pixel count	Mean (SD)	Atlas label
Control	161	1.248 (1.134)	cerebel_Left_VI
	1368	12.202 (3.990)	cerebel_Left_Crus_I
	83	16.912 (8.980)	inf_fronto-occip-fasciculus_L
	1051	27.392 (9.275)	inf_long_fasciculus_L
	1252	29.034 (8.010)	sup_long_fasciculus_L
	110	21.40 (8.064)	sup_long_fasciculus_temp_L
Dysgraphic	356	1.068 (1.156)	cerebel_Left_VI
	2381	8.450 (3.921)	cerebel_Left_Crus_I
	581	5.646 (3.444)	inf_fronto-occip-fasciculus_L
	2576	15.545 (6.079)	inf_long_fasciculus_L
	2052	19.718 (6.771)	sup_long_fasciculus_L
	267	11.394 (5.881)	sup_long_fasciculus_temp_L
Dyslexic	2055	8.735 (3.793)	cerebel_Left_Crus_I
	119	12.730 (4.224)	inf_fronto-occip-fasciculus_L
	1341	20.905 (7.057)	inf_long_fasciculus_L
	1766	19.353 (7.519)	sup_long_fasciculus_L
	189	12.306 (5.890)	sup_long_fasciculus_temp_L
Left precuneus seed point.			
Subject group	Pixel count	Mean (SD)	Atlas label
Control	270	0.052 (0.068)	cerebel_Left_I-IV
	97	0.006 (0.010)	cerebel_Right_I-IV
	5962	0.461 (0.384)	L ant thal rad
	168	1.50 (1.060)	R ant thal rad
	6732	0.029 (0.036)	L cort spinal
	5272	19.602 (6.812)	L cingulum
	334	2.150 (1.517)	R cingulum
	2259	3.244 (2.030)	L cing hippo
	309	0.022 (0.040)	R cing hippo
	6228	0.428 (0.253)	forceps major
	3946	0.063 (0.083)	inf_fronto-occip-fasciculus_L
	99	0.002 (0.005)	inf_fronto-occip-fasciculus_R
	5276	0.164 (0.176)	inf_long_fasciculus_L
	7604	0.017 (0.019)	sup_long_fasciculus_L
	247	0.022 (0.048)	sup_long_fasciculus_temp_L

(continued on next page)

Table 6 (continued)

Left precuneus seed point.				
Subject group	Pixel count	Mean (SD)	Atlas label	
Dysgraphic	203	15.653 (16.437)	L ant thal rad	
	5214	21.109 (11.979)	L cingulum	
	288	3.370 (2.677)	R cingulum	
	818	9.218 (5.935)	L cing hippo	
	390	5.326 (5.996)	forceps major	
	56	15.711 (20.295)	inf_long_fasciculus_L	
	Dyslexic	169	9.207 (6.695)	L ant thal rad
		4087	21.589 (8.070)	L cingulum
		221	2.924 (2.364)	R cingulum
		240	11.115 (4.281)	L cing hippo
63		9.273 (8.566)	forceps major	
145		6.941 (7.670)	inf_long_fasciculus_L	
Left supramarginal gyrus seed point.				
Subject group	Pixel count	Mean (SD)	Atlas label	
Control	101	0.546 (0.708)	L cingulum	
	72	6.013 (5.622)	inf_long_fasciculus_L	
Dysgraphic	4752	36.919 (7.50)	sup_long_fasciculus_L	
	3044	1.049 (1.146)	L ant thal rad	
	992	0.005 (0.007)	R ant thal rad	
	2906	4.603 (4.377)	L cort spinal	
	2014	0.007 (0.012)	R cort spinal	
	115	0.028 (0.040)	L cingulum	
	201	0.009 (0.016)	L cing hippo	
	1437	0.109 (0.189)	forceps major	
	489	0.588 (0.855)	inf_fronto-occip-fasciculus_L	
	621	0.50 (0.802)	inf_long_fasciculus_L	
	17,352	20.236 (8.761)	sup_long_fasciculus_L	
	Dyslexic	3835	2.535 (3.214)	L ant thal rad
1487		0.004 (0.005)	R ant thal rad	
4498		2.705 (2.246)	L cort spinal	
2321		0.005 (0.007)	R cort spinal	
1203		0.292 (0.406)	L cingulum	
997		0.011 (0.012)	forceps major	
1250		1.223 (1.576)	inf_fronto-occip-fasciculus_L	
2118		0.626 (0.722)	inf_long_fasciculus_L	
19,773		17.105 (7.311)	sup_long_fasciculus_L	
98		1.261 (1.689)	sup_long_fasciculus_temp_L	
Left Broca's inferior frontal seed point.				
Subject group	Pixel count	Mean (SD)	Atlas label	
Control	9148	4.203 (3.053)	L ant thal rad	
	3728	1.227 (1.403)	L cingulum	
	18081	0.503 (0.710)	forceps minor	
	7010	5.333 (3.324)	inf_fronto-occip-fasciculus_L	
	3064	0.001 (0.002)	inf_long_fasciculus_L	
	15,538	4.326 (2.428)	sup_long_fasciculus_L	
	3113	3.045 (2.252)	L uncinata	
	161	0.576 (0.302)	sup_long_fasciculus_temp_L	
	232	0.230 (0.382)	sup_long_fasciculus_temp_R	
	Dysgraphic	1926	17.228 (9.694)	L ant thal rad
323		1.30 (1.644)	L cingulum	
756		4.322 (6.695)	forceps minor	
1688		20.101 (8.079)	inf_fronto-occip-fasciculus_L	
2724		17.663 (5.536)	sup_long_fasciculus_L	
421		15.337 (7.301)	L uncinata	
Dyslexic	417	23.508 (7.071)	L ant thal rad	
	841	19.934 (5.739)	inf_fronto-occip-fasciculus_L	
	2346	14.742 (6.389)	sup_long_fasciculus_L	
	158	14.785 (5.580)	L uncinata	

### 3.4. Examples of contrasting patterns of neurological profiles in dysgraphia and dyslexia

Fig. 1 shows the anatomical locations of both the fMRI connectivity and DTI parameter (relative anisotropy, ratio of uni-directional to multi-directional diffusivity) differences between the control and dysgraphia groups. Fig. 2 shows the anatomical locations of both the fMRI connectivity and DTI (radial perpendicular diffusivity) parameter differences between the dyslexia and dysgraphia groups. Fig. 3 shows a scatter plot for the correlation between DTI RA and fMRI functional

connectivity on the alphabet task for the dyslexia group from one seed point.

## 4. Discussion

### 4.1. Findings related to white matter integrity

Patterns of how dysgraphics differed from controls, dyslexics differed from controls, and dysgraphics and dyslexics differed on each of four DTI indices varied depending on which of the four DTI indices of

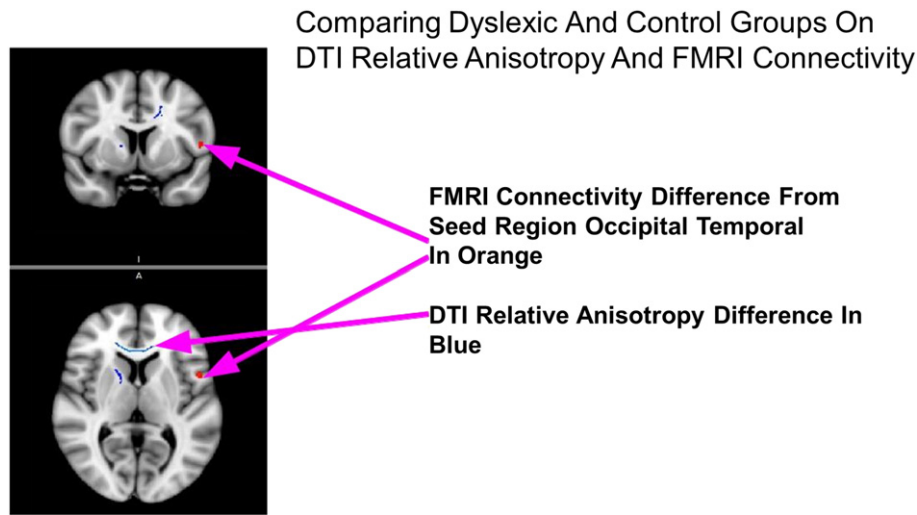


**Fig. 1.** Top panel—coronal view, bottom panel—axial view. Functional connectivity and structural white matter integrity connectivity where there was a significant difference between the control and dysgraphia groups. The area in orange shows where the dysgraphic group had greater fMRI connectivity than the control group to a seed region in the left occipito-temporal region. The regions in blue/light blue show where the control group had greater relative anisotropy (DTI parameter similar to fractional anisotropy) than dysgraphic group. The language-related pathways involving the right anterior thalamic radiation and the forceps minor are visible in the blue highlighted region. The image is in radiological orientation.

white matter integrity was analyzed. Only the dysgraphic group differed from control group on fractional anisotropy (FA), which may be associated with myelination (Wheeler-Kingshott et al., 2009; Mori, 2007). Only the dyslexia group differed from the control group on parallel axial diffusivity (AD), which may be related to axon diameter (Song, 2002; Song, 2005). On relative anisotropy (RA), the dysgraphic and dyslexic groups differed from the control group on four common regions, but differed from the control group in contrasting ways in six other regions, five of which differentiated the dyslexic group from the control group. The dysgraphic and dyslexic groups differed from each other bilaterally on perpendicular radial diffusivity (RD) in seven fiber tracts. Thus, overall the dysgraphic and dyslexic groups differed from each other and from the control group in white matter integrity in contrasting ways.

Findings for specific DTI indicators may have clinical significance. RA results for greater bilateral anterior thalamic radiation in the control group compared to the dysgraphia group or dyslexia group make sense in light of research showing relationships between thalamic connectivity and ADHD (Xia, 2012) and evidence of impaired supervisory attention in dysgraphia and dyslexia (Berninger and Richards, 2010). Results for greater left cingulum white matter integrity in the control group compared to the dysgraphic group or the dyslexic group are consistent with the well-documented role of the cingulum in executive functions in both handwriting and spelling skills and impaired executive functions in dysgraphia and dyslexia (Berninger and Richards, 2010). The findings for greater forceps minor white matter integrity in the frontal portion of the corpus callosum connecting with the prefrontal cortex in the control group than in the dysgraphic group or dysgraphic group are consistent with the frequent research finding of working memory problems in dysgraphia and dyslexia (Berninger and Richards, 2010).

Of interest, only the dyslexia group showed less RA compared to the control group in bilateral IFOF, which connects posterior and anterior language systems, and the uncinata, which is a late maturing limbic-cortical pathway. Also of interest, on RA the dysgraphic group differed from the control group in the left cortical spinal tract, but the dyslexic group differed from the control group in right cortical spinal tract. A possible explanation for this lateral difference is that the right-handed participants with dysgraphia lack white matter integrity on the contralateral cortical spinal tract, which interferes with letter production by their dominant hand, whereas the participants with dyslexia lack white matter integrity on the right cortical tract (projecting to the left

visual field) which may interfere with foveal vision during eye movements from left to right while reading or spelling a word. Further evidence of contrasting patterns of white matter integrity between dyslexia and dysgraphia was the greater RD (perpendicular diffusion) in seven brain regions on the right in the dyslexic group but left in the dysgraphic group.

The number and patterns of probabilistic tractography connections for the DTI seed point analysis also identified contrasting patterns of white matter integrity. From the occipital temporal seed point, the dysgraphia group did not differ from the control group, and the dyslexic group differed from control group only in connection to the left cerebellum. However, from the precuneus cortex and inferior frontal gyrus (Broca's) seed points, the control group had many more DTI findings than did either the dysgraphia group or dyslexia group, but the dysgraphia and dyslexic groups did not have exactly the same DTI findings. From the supramarginal gyrus seed point, the control group had only two DTI findings, but the dysgraphia and dyslexia groups had many more, but not exactly the same ones. Overall, the control group showed more white matter integrity than either the dysgraphic or dyslexic groups, but two kinds of DTI differences were observed in those groups—less white matter integrity from the precuneus cortex and inferior frontal gyrus seed points or more white matter integrity from the SMG seed point. However, overall the seed points from the metaanalysis of brain regions involved in written word production (Purcell, 2011) captured the contrasting neurobiological patterns differentiating the control from the dysgraphic or dyslexic groups.

Collectively the DTI findings show contrasting profiles of white matter integrity in dysgraphia and dyslexia. Whereas the dysgraphics differed from controls in DTI FA which is thought to be associated with amount of myelination (Wheeler-Kingshott et al., 2009; Mori, 2007), the dyslexics differed from controls in DTI RA, also thought to be associated with the amount of myelination (Basser and Pierpaoli, 1996), DTI AD, which is parallel diffusion which is thought to be related to axon diameter (Song, 2002; Song, 2005), and DTI RD, which is perpendicular diffusion and is thought to be related to the degree of myelination (Song, 2002; Song, 2005).

#### 4.2. Findings related to fMRI functional connectivity

Although the dysgraphia group did not differ from the control group on the alphabet writing task in functional connectivity, the pattern of

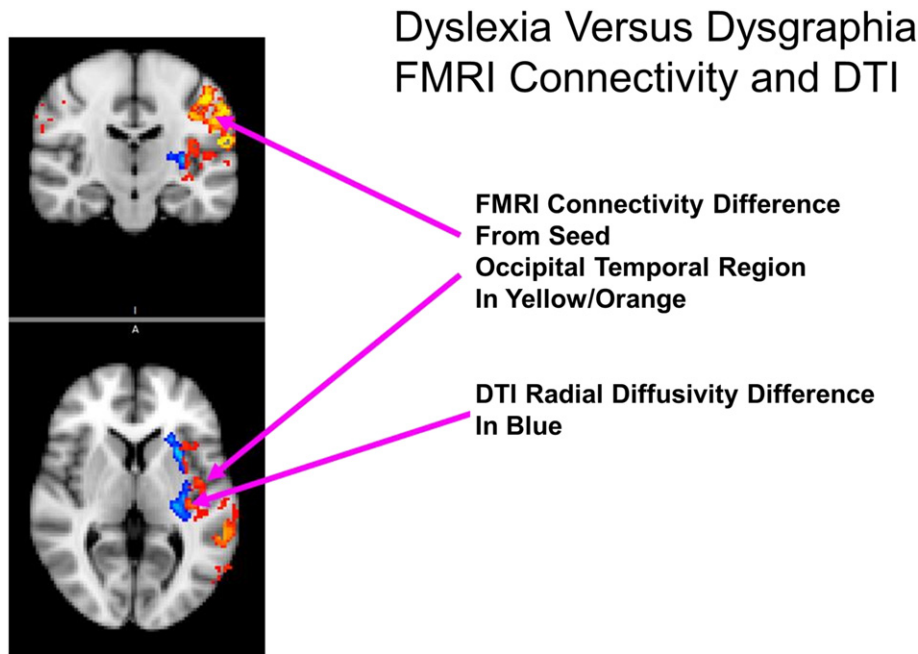


**Fig. 2.** Top panel—coronal view, bottom panel—axial view. Functional connectivity and structural white matter integrity connectivity where there was a significant difference between the dyslexia and dysgraphia groups. The clusters in yellow/orange show where the dyslexic group had greater connectivity, compared to the dysgraphic group in fMRI connectivity, to a seed region in the occipito-temporal region. The clusters in blue/light blue show where the dysgraphic group had greater radial diffusivity (RD) than the dyslexic group. Notice the anatomic concordance of the fMRI connectivity and the DTI parameter clusters on the left side of the brain. The language-related pathways involving the anterior thalamic radiation (white matter tract) and the inferior parietal cortex (gray matter) shown in this figure are both heavily involved in language processing. The image is in radiological orientation.

functional connectivity on the alphabet letter writing task was different for the dysgraphia group and the dyslexia group. The dysgraphia group showed more functionally connected voxels from the left precuneus, a region common to both the default network and Rich Club of the Human Connectome (Bullmore and Sporns, 2009; Smith, 2013; van den Heuvel and Sporns, 2011) than the dyslexia group; but the dyslexia group showed more functionally connected voxels from the left occipital temporal and left supramarginal gyri. Thus, there may be contrasting patterns of functional connectivity for the same alphabet

writing task between dysgraphia (impaired handwriting) and dyslexia (impaired word spelling/reading). A possible explanation, based on overconnectivity from the precuneus in children with dysgraphia, is that children with persisting handwriting problems lack awareness of letter form or of alphabet order, which in turn interferes with subword level of written language on the alphabet writing task. Another possible explanation is that for children with dyslexia their problems in writing the alphabet from memory are more related to automatic letter formation, as assessed by comparing real letter and pseudoletter writing in a prior but not the current study (Richards, 2011) than to finding the letter in the ordered alphabet. In contrast, the children with persisting dyslexia showed functional overconnectivity in a region where visual inputs are first processed as letters in visible language (left occipital temporal gyrus) supported by working memory (left supramarginal gyrus). Thus, there appears to be a different neural basis for letter writing on the alphabet writing task for the dysgraphic and dyslexic groups.

In addition, it is not surprising that on the spelling task the dyslexia group had more functionally connected voxels for all four seed points than the dysgraphia group, consistent with dyslexia being associated with impaired word spelling. The dyslexia group had greater functional connectivity than the control group, especially to the cerebellum, on both written language tasks. Over-connectedness with the cerebellar regions may explain the frequently reported inefficiencies in neural timing of language processing in dyslexia (Berninger and Richards, 2010).

It was surprising that, compared to the control group, the dysgraphic and dyslexic groups differed in contrasting ways on two kinds of cognitive tasks related to writing, but not assessed on conventional measures of intellectual function. Specifically, the dysgraphic group showed more functional connections from three seed points (all but left supramarginal gyrus) than the control group or dyslexic group on planning for composing; but the dyslexic group showed more functional connections during flow in the resting condition compared to the controls from one seed point (left occipital temporal gyrus). However, when the dyslexic and dysgraphic groups were compared to each other the pattern of overconnectivity changed from that for comparison

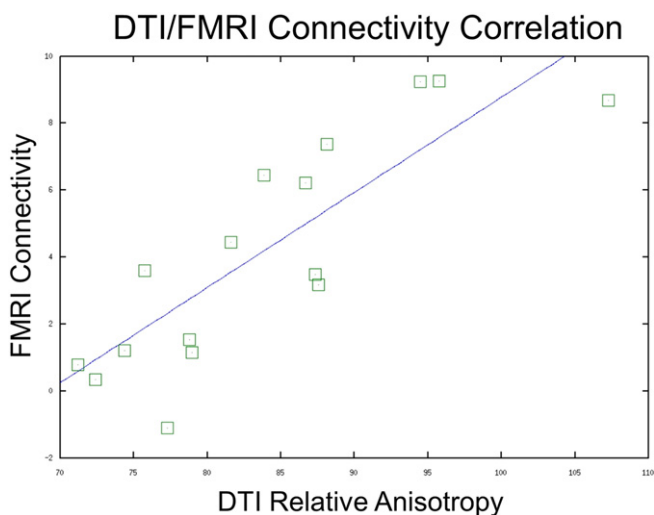


**Fig. 3.** Scatter plot of DTI relative anisotropy (RA) versus fMRI connectivity on the alphabet task for the dyslexia group from one seed point. Each box on the plot comes from an individual subject using their value of DTI RA (extracted from MNI coordinates 32,17, 35 mm where there was a significant difference between the dyslexic group and the control group) and fMRI connectivity value (within the left angular gyrus). This plot shows a positive correlation between DTI and fMRI connectivity with an  $r$  correlation value of 0.84 ( $p < 0.01$ ).

with controls. For both mind wandering during rest and planning for composing, the dysgraphics showed more functional connectivity from all four seed points.

Thus, the first hypothesis was supported, in part: the dysgraphic and dyslexic groups differed from each other in functional connectivity on tasks that contrasted in level of language associated with their hallmark impairments—letter production in alphabetic order out of word context in dysgraphia or letter production in word context in dyslexia. However, it was not a simple story of the dysgraphic group differing from the control group only on the alphabet writing task, and the dyslexic group differing from the control group only on the spelling task. Rather, the dysgraphic group differed from the dyslexic group on the alphabet writing task from one seed point that may be related to linguistic awareness for letter forms and their positions in the ordered alphabet. The hypothesis was supported in that the dyslexic group differed from the control group and from the dysgraphic group on the spelling task, when the task was to write a letter to complete the word-specific spelling rather than make a yes/no judgment about whether a letter string is a correct word-specific spelling response requirement. However, the dyslexic group also differed from the control group and dysgraphic group on the alphabet writing task from some seed points, but not the same one as the dysgraphic group did.

However, the second hypothesis was not supported. The dysgraphic group and dyslexic groups differed from the control group on cognitive tasks, but in contrasting ways. That the dysgraphia group did not differ from the control group during resting condition (Vaden et al., 2015) is consistent with the view that dysgraphics have normal cognitive flow of thoughts when not constrained by planning for an externally imposed goal. That the dysgraphia group did differ from the control group on the planning task when a topic was provided to them is consistent with the impaired supervisory attention functions in working memory for planning often observed in dysgraphia (Berninger and Richards, 2010). The dyslexia group's stronger functional connectivity than the control group during resting state (mind wandering) is consistent with dyslexia being associated with difficulties in self-regulation when managing their own learning without teacher guidance and support. That the dyslexia group did not differ from the control group in functional connectivity during planning is consistent with their ability to benefit from teacher provided guidance and support, for example, in providing a topic to write about (what) as well as a reason for it (why), as was included in instructions.

Also of interest is the number of connections observed from cortical seed points to the left and/or right uncinate fasciculus in the limbic system (see Tables 2 and 6). The uncinate fasciculus is the last fiber tract to mature (Hasan et al., 2009) and its function is not fully understood. However, a possible implication of uncinate involvement is that for children with dysgraphia and dyslexia handwriting and spelling should be taught systematically beyond the early grades continuing in grades 4–9 because a relevant white fiber tract may still be maturing during the upper elementary and middle school grades. Future research should also investigate the connections between social/emotional/motivational functions in the limbic system and cognitive/linguistic functions in the cortex for learning to write and read for both typical language learners and those with dysgraphia or dyslexia.

Overall, the findings (a) show the importance of comparing patterns both to controls and to other specific written learning disabilities in drawing conclusions relevant to differential diagnosis; and (b) serve as a reminder that impaired handwriting or spelling may be associated with both cognitive and language problems. Handwriting is not just a motor skill or just a language skill.

#### 4.3. Findings for white matter–gray matter correlations

Unexpectedly, both correlations between white matter integrity (FA) and gray matter functional connectivity for dysgraphia were on

the spelling task on which children had to write a missing letter to create a word specific spelling. This result supports the frequent clinical observation that children with primary impairment in handwriting often have associated spelling problems without reading problems. Moreover, the connections from the seed points in the supramarginal gyrus to the anterior cingulate and from seed points in the inferior frontal gyrus to the frontal gyrus are consistent with findings for word-specific spelling in children with dysgraphia in an fMRI BOLD study (Richards, 2009).

Also unexpectedly, for both DTI RA and DTI AD, the dyslexics showed impairment on both the alphabet writing task and fill in the blank to create a correct word spelling task. These findings are consistent with evidence that (a) children with dyslexia have difficulty with finding, accessing, and producing letters in alphabetic order due to an impaired orthographic loop in working memory for integrating access to letter codes with producing them through sequential finger movements (Berninger and Richards, 2010); and (b) letter production impairments in dysgraphia and dyslexia are not the same even when dyslexia and dysgraphia co-occur (Alstad et al., 2015).

Clearly, the dysgraphic and dyslexic groups showed different patterns of DTI–fMRI connectivity correlations for DTI parameters on which the control group differed from the dysgraphia and/or dyslexia groups. Some white matter–gray matter correlations may be hallmark contributors to the behavioral manifestation of dysgraphia versus dyslexia, whereas lack of such correlations may also be contributing factors and related to specific DTI under-connectivity or fMRI over-connectivity that can interfere with the necessary white matter–gray matter connections forming. For example, although no significant DT RD–fMRI connections were found for the written language tasks, clearly the dysgraphic and dyslexic groups differ in DT RD in seven locations. See Fig. 2.

#### 4.4. Complex connectome supporting writing

Collectively, the current findings provide evidence for contrasting neurobiological patterns during two written language tasks for typical writing development, developmental dysgraphia and developmental dyslexia during middle childhood and early adolescence. Overall, controls tended to have more indicators of structural white matter integrity, and fewer functional connections, consistent with more efficient processing on written language tasks at the subword and word levels. In contrast, those with dysgraphia or dyslexia had fewer indicators of structural white matter integrity, but considerably more fMRI functional connections, consistent with inefficiency in orchestrating the mind for writing-related language or cognitive tasks. However, the DTI indicators, fMRI functional connections, and the DTI–fMRI connection correlations were not identical across dysgraphia and dyslexia. For example, there were not only significant differences in DTI white matter integrity between the dysgraphic and dyslexic groups in the left inferior fronto-occipital fasciculus (IFOF) and left superior longitudinal fasciculus (SLF), but also differences in fMRI functional connectivity to the inferior parietal lobule from the occipital temporal seed point. Martino et al. (2010) showed that the IFOF has cortical terminations in the parietal, occipital and temporal lobes, which are involved in semantic processing; and semantics contributes to word-specific spelling. Catani et al. (2005) showed that beyond the arcuate pathway connecting Broca's and Wernicke's areas, there was another pathway passing through the inferior parietal cortex connecting the inferior parietal lobe to Wernicke's territory; both are involved in word reading and spelling.

One potential explanation of functional over-connectivity of the dysgraphic or dyslexic groups compared to the control group is neural inefficiency. The functional inefficiency may be related to the lack of the structural white matter integrity observed in the dysgraphic and dyslexic groups compared to the control group on multiple DTI indices. Functional over-connectivity may be a compensation mechanism.

Another possibility is that the functional inefficiency may be related to genetic mechanisms. Although much has been learned about the genetic bases of dyslexia (Schulte-Körne, 1998; Berninger and Richards, 2010), less research has been directed to the genetic bases of dysgraphia. However, these two possibilities are not mutually exclusive as genetic mechanisms that regulate neural development may contribute to the white matter differences and neural inefficiency. What is clear from the current study is that dysgraphia and dyslexia differ from controls and each other not only on behavioral measures but also on brain indices of DTI structural and fMRI functional connectivity. On the one hand, for dysgraphia DTI FA correlations were significant from one posterior seed point (supramarginal gyrus) and one anterior seed point (inferior frontal gyrus) during the fill in the blank during spelling task. On the other hand, for dyslexia, DTI RA–fMRI functional connectivity correlations were significant from two posterior seed points (occipitotemporal and supramarginal gyri) and one anterior seed point (inferior frontal gyrus) during alphabet writing and from one posterior seed point (occipitotemporal gyrus) and one anterior seed point (inferior frontal gyrus) during the fill in the blank during spelling task.

The current study adds to the rapidly expanding knowledge of the heavily connected brain (van den Heuvel and Sporns, 2011; Markov et al., 2013a; Markov et al., 2013b; Stern, 2013) by showing that structural connections and functional connections are related in differential and complex ways in children with and without dysgraphia and dyslexia. Whether more white matter integrity and less functional connectivity, as observed in the control group, is adaptive, is unknown. Answering this question warrants future research and the answer, like the human brain, may be complex.

#### 4.5. Clinical significance

During the Common Core era in the US (Common Core, 2013), writing disabilities, which epidemiological research shows affect a sizable number of school age-children, are the forgotten Specific Learning Disability (SLD) (Katusic et al., 2009). Neuroscience research has an important societal contribution to make in educating educators and policy makers that these brain-based SLDs affecting writing – dysgraphia and dyslexia – exist, can be diagnosed, have different brain bases (as the plural suffix on specific learning disabilities indicates), and deserve individually tailored instruction because they are not neurologically or behaviorally identical. Moreover, the handwriting and spelling problems may persist beyond the early grades and systematic, explicit instruction in handwriting and spelling may be needed during middle childhood and adolescence. The current research shows that appropriate instruction for remediating dysgraphia and dyslexia should be directed to cognitive as well as language processes.

#### Acknowledgments

The current study, supported by grant P50HD071764 from the Eunice Kennedy Shriver National Institute of Child Health and Human Development (NICHD) at the National Institutes of Health (NIH) to the University of Washington Learning Disabilities Research Center, has been an interdisciplinary team effort. The authors also thank Liza Young for the help with subject coordination, Tara Madhyastha for the help with the white matter regressor filter, Tim Wilbur for the help with MR scanning, Frederick (Fritz) Reitz for developing the MRI-compatible pen, and Elliot Collins for the initial help with software pipeline.

#### References

Alstad, Z., et al., 2015. Modes of alphabet letter production during middle childhood and adolescence: interrelationships with each other and other writing skills. *Journal of Writing Research* 6 (3), 199–231.

Barnett, A., et al., 2007. *Detailed Assessment of Speed of Handwriting (DASH) Copy Best and Fast*. Pearson, London.

Basser, P.J., Pierpaoli, C., 1996. Microstructural and physiological features of tissues elucidated by quantitative-diffusion-tensor MRI. *J. Magn. Reson. B* 111 (3), 209–219. <http://dx.doi.org/10.1006/jmrb.1996.00868661285>.

Berninger, V., Richards, T., 2010. Inter-relationships among behavioral markers, genes, brain, and treatment in dyslexia and dysgraphia. *Future Neurol.* 5, 597–617.

Berninger, V.W., et al., 2009. fMRI activation related to nature of ideas generated and differences between good and poor writers during idea generation. *British Journal of Educational Psychology Monograph Series* 2 (6), 77–93.

Bruck, M., 1993. Component spelling skills of college students with childhood diagnoses of dyslexia. *Learning Disability Quarterly* 16 (3), 171–184. <http://dx.doi.org/10.2307/1511325>.

Bullmore, E., Sporns, O., 2009. Complex brain networks: graph theoretical analysis of structural and functional systems. *Nat. Rev. Neurosci.* 10 (3), 186–198. <http://dx.doi.org/10.1038/nrn257519190637>.

Caspers, S., et al., 2013. Organization of the human inferior parietal lobule based on receptor architectonics. *Cereb. Cortex* 23 (3), 615–628. <http://dx.doi.org/10.1093/cercor/bhs04822375016>.

Catani, M., et al., 2005. Perisylvian language networks of the human brain. *Ann. Neurol.* 57 (1), 8–16. <http://dx.doi.org/10.1002/ana.2031915597383>.

Common Core, 2013. <http://www.corestandards.org/Standards/index.htm>.

Connelly, V., et al., 2006. Contribution of lower order skills to the written composition of college students with and without dyslexia. *Dev Neuropsychol* 29 (1), 175–196. [http://dx.doi.org/10.1207/s15326942dn2901\\_916390293](http://dx.doi.org/10.1207/s15326942dn2901_916390293).

Eickhoff, S.B., et al., 2005. A new SPM toolbox for combining probabilistic cytoarchitectonic maps and functional imaging data. *Neuroimage* 25 (4), 1325–1335. <http://dx.doi.org/10.1016/j.neuroimage.2004.12.03415850749>.

Eickhoff, S.B., et al., 2006. Testing anatomically specified hypotheses in functional imaging using cytoarchitectonic maps. *Neuroimage* 32 (2), 570–582. <http://dx.doi.org/10.1016/j.neuroimage.2006.04.20416781166>.

Eickhoff, S.B., et al., 2007. Assignment of functional activations to probabilistic cytoarchitectonic areas revisited. *Neuroimage* 36 (3), 511–521. <http://dx.doi.org/10.1016/j.neuroimage.2007.03.06017499520>.

Hasan, K.M., et al., 2009. Development and aging of the healthy human brain uncinate fasciculus across the lifespan using diffusion tensor magnetic resonance imaging. *Brain Res.* 1276, 67–76. <http://dx.doi.org/10.1016/j.brainres.2009.04.02519393229>.

Hayes, J.R., A new model of cognition and affect in writing. In: M. Levy, S. Ransdell (Eds.). *The Science of Writing* (1996). Erlbaum, Hillsdale, NJ.

Jenkinson, M., et al., 2002. Improved optimization for the robust and accurate linear registration and motion correction of brain images. *Neuroimage* 17 (2), 825–841. <http://dx.doi.org/10.1006/nimg.2002.113212377157>.

Katusic, S.K., et al., 2009. The forgotten learning disability – epidemiology of written language disorder in a population-based birth cohort (1976–1982), Rochester, Minnesota. *Pediatrics* 123 (5), 1306–1313.

Kellogg, R., 1994. *Psychology of Writing*. Oxford University Press, New York.

Klingberg, T., et al., 2000. Microstructure of temporoparietal white matter as a basis for reading ability: evidence from diffusion tensor magnetic resonance imaging. *Neuron* 25 (2), 493–500. [http://dx.doi.org/10.1016/S0896-6273\(00\)80911-310719902](http://dx.doi.org/10.1016/S0896-6273(00)80911-310719902).

Lefly, D., Pennington, B., 1991. Spelling errors and reading fluency in dyslexics. *Annu. Dys* 41, 143–162.

Markov, N., et al., 2013a. Introduction to and contents in the special section on the heavily connected brain. *Science* 342, 577–589.

Markov, N.T., et al., 2013b. Cortical high-density counterstream architectures. *Science* 342 (6158), 1238406. <http://dx.doi.org/10.1126/science.123840624179228>.

Martino, J., et al., 2010. Anatomic dissection of the inferior fronto-occipital fasciculus revisited in the lights of brain stimulation data. *Cortex* 46 (5), 691–699. <http://dx.doi.org/10.1016/j.cortex.2009.07.01519775684>.

Mather, N., et al., 2008. *Test of Orthographic Competence (TOC)*. Pro-Ed, Austin, TX.

Mori, S., 2007. *Introduction to Diffusion Tensor Imaging*. Elsevier, Amsterdam.

Olesen, P.J., et al., 2003. Combined analysis of DTI and fMRI data reveals a joint maturation of white and grey matter in a fronto-parietal network. *Brain Res Cogn Brain Res* 18 (1), 48–57. <http://dx.doi.org/10.1016/j.cogbrainres.2003.09.00314659496>.

Olson, R. et al., Measurement of word recognition, orthographic, and phonological skills. In: G.R. Lyon (Ed.). *Frames of Reference for the Assessment of Learning Disabilities* (1994). Brooks, Baltimore.

Pearson, 2009. *Wechsler Individual Achievement Test third edition*. Pearson, San Antonio, TX.

Purcell, J.J., et al., 2011. Examining the central and peripheral processes of written word production through meta-analysis. *Front. Psychol.* 2, 239. <http://dx.doi.org/10.3389/fpsyg.2011.0023922013427>.

Raichle, M.E., et al., 2001. A default mode of brain function. *Proc. Natl. Acad. Sci. U. S. A.* 98 (2), 676–682. <http://dx.doi.org/10.1073/pnas.98.2.67611209064>.

Reitz, F., et al., 2013. A low-cost, computer-interfaced drawing pad for fMRI studies of dysgraphia and dyslexia. *Sensors (Basel)* 13 (4), 5099–5108. <http://dx.doi.org/10.3390/s13040509923595203>.

Richards, T., et al., 2006. Individual fMRI activation in orthographic mapping and morpheme mapping after orthographic or morphological spelling treatment in child dyslexics. *J. Neuroling.* 19 (1), 56–86.

Richards, T.L., et al., 2009. fMRI activation differences between 11-year-old good and poor spellers' access in working memory to temporary and long-term orthographic representations. *Journal of Neurolinguistics* 22 (4), 327–353. <http://dx.doi.org/10.1016/j.jneuroling.2008.11.002>.

Richards, T.L., et al., 2011. Differences between good and poor child writers on fMRI contrasts for writing newly taught and highly practiced letter forms. *Read Writ* 24 (5), 493–516. <http://dx.doi.org/10.1007/s11145-009-9217-3>.

- Richards, T.L., Berninger, V.W., 2008. Abnormal fMRI connectivity in children with dyslexia during a phoneme task: before but not after treatment. *Journal of Neurolinguistics* 21 (4), 294–304. <http://dx.doi.org/10.1016/j.jneuroling.2007.07.002>.
- Schulte-Körne, G., et al., 1998. Evidence for linkage of spelling disability to chromosome 15. *Am. J. Hum. Genet.* 63 (1), 279–282. <http://dx.doi.org/10.1086/3019199634517>.
- Smith, S., 2013. Introduction to the NeuroImage special issue "Mapping the Connectome". *Neuroimage* 80, 1. <http://dx.doi.org/10.1016/j.neuroimage.2013.07.01223870176>.
- Song, S.K., et al., 2002. Demyelination revealed through MRI as increased radial (but unchanged axial) diffusion of water. *Neuroimage* 17 (3), 1429–1436. <http://dx.doi.org/10.1006/nimg.2002.126712414282>.
- Song, S.K., et al., 2005. Demyelination increases radial diffusivity in corpus callosum of mouse brain. *Neuroimage* 26 (1), 132–140. <http://dx.doi.org/10.1016/j.neuroimage.2005.01.02815862213>.
- Stern, P., 2013. The heavily connected brain. *Connection, connection, connection...* Introduction. *Science* 342 (6158), 577. <http://dx.doi.org/10.1126/science.342.6158.57724179217>.
- Toga, A.W., et al., 2006. Towards multimodal atlases of the human brain. *Nat. Rev. Neurosci.* 7 (12), 952–966. <http://dx.doi.org/10.1038/nrn201217115077>.
- Vaden, K.I., Kuchinsky, S.E., Ahlstrom, J.B., Dubno, J.R., Eckert, M.A., 2015. Cortical activity predicts which older adults recognize speech in noise and when. *J. Neurosci.* 35, 3929–3937. <http://dx.doi.org/10.1523/JNEUROSCI.2908-14.201525740521>.
- van den Heuvel, M., Sporns, O., 2011. Rich-club organization of the human connectome. *J. Neurosci.* 44, 15775–15786.
- Vandermosten, M., et al., 2012. A tractography study in dyslexia: neuroanatomic correlates of orthographic, phonological and speech processing. *Brain* 135 (3), 935–948. <http://dx.doi.org/10.1093/brain/awr36322327793>.
- Wheeler-Kingshott, C.A.M., Cercignani, M., 2009. About "axial" and "radial" diffusivities. *Magn. Reson. Med.* 61 (5), 1255–1260. <http://dx.doi.org/10.1002/mrm.21965>.
- Xia, S., et al., 2012. Thalamic shape and connectivity abnormalities in children with attention-deficit/hyperactivity disorder. *Psychiatry Res* 204 (2–3), 161–167. <http://dx.doi.org/10.1016/j.psychres.2012.04.01123149038>.